Stochastic Modeling for the Aggregated Flexibility of Distributed Energy Resources

Yilin Wen*, Yi Guo†‡, Zechun Hu*, Gabriela Hug†
*Department of Electrical Engineering, Tsinghua University, Beijing, China
wen-yl20@mails.tsinghua.edu.cn, zechhu@tsinghua.edu.cn
†Power Systems Laboratory, ETH Zürich, Zürich, Switzerland
guo@eeh.ee.ethz.ch;hug@eeh.ee.ethz.ch
‡Urban Energy Systems Laboratory, Empa, Dübendorf, Switzerland
yi.guo@empa.ch

***Abstract*—This paper proposes an uncertainty modeling method for the aggregated power flexibility of DERs. Basically, both outer and inner approximated power-energy boundary models are utilized to describe the aggregated flexibility of controllable DERs. These power and energy boundary parameters are uncertain because the availability of controllable devices, such as electric vehicles and thermostatically controlled loads, cannot be precisely predicted. The optimal operation problem of the aggregator is thus formulated as chance-constrained programming (CCP). Then, a flexibility envelope searching algorithm based on the ALSO-X+ method is proposed to solve the CCP, the result of which is a conservative approximation of the original CCP but not as conservative as the Conditional Value-at-Risk approximation. After optimizing the aggregated power of the group of DERs, the decision at the aggregator level is disaggregated into the flexibility regions of individual DERs. Finally, the numerical test demonstrates the effectiveness and robustness of the proposed method.**

***Index Terms*—Aggregated flexibility, chance-constrained programming, distributed energy resources, flexibility modeling and identification, uncertainty modeling.**

I. Introduction

Renewable energy generations, such as wind and solar power, are increasingly integrated into power systems for environmental concerns and sustainability [1]. The intermittent nature of these renewable energies poses challenges to the electricity supply and demand balance and, thus, increases the need for flexibility in the power system operation. In this context, flexibilities provided by demand-side distributed energy resources (DERs), e.g., electric vehicles (EVs), distributed energy storage systems (DESSs), rooftop photovoltaics (PVs), and heating, ventilation, and air conditioning systems (HVACs), are expected to play a critical role in future power systems [2]. The flexibility, or the so-called operational range, of a DER refers to the feasible region of its power output. In the rest of this paper, we limit the term "power" to active power since it is the main quantity for dispatch decisions and market strategies. Unlike conventional generators, the flexibilities of DERs are affected by various uncertain factors, such as the arrival and departure times of EVs [3] and the ambient temperature of HVACs [4]. Therefore, it is important to consider the uncertainty modeling of these small-scale flexibility providers to leverage their potential flexibility to enhance the security, economic efficiency, and robustness of power systems operation with high penetration of renewables.

Small-scale DERs are usually dispatched in an aggregated fashion due to their limited capacities [5], [6]. The identification of their flexibility, thereby, is affected by the autonomous operational patterns of individual DERs, which are heterogeneous and hard to predict. Therefore, it is important to include the uncertainty modeling of the flexibility of DERs for the day-ahead/hour-ahead operation of the DERs' decision-maker, e.g., the aggregator, the power market operator, or the dispatch center. This uncertainty modeling aims to ensure that an optimal and robust dispatch decision at an aggregation level can also be feasible for the operational constraints of individual DERs. Along this direction, there are two research lines to address the flexibility identification of DERs with modeling uncertainty: the first is to derive stochastic models of individual DERs [7], [8] and then aggregate these models; another line of research develops a deterministic aggregated flexibility model and then introduces stochasticity into this model, which is studied in this paper.

The reasons for choosing the second approach are as follows. The uncertainty modeling of flexibility relies on the prediction of parameters that are used to describe the flexibility model. Predicting the flexibility of individual Distributed Energy Resources (DERs) is challenging due to their operation's inherent randomness. For instance, the timing of EVs connecting to chargers is determined by the unpredictable travel demands of the owners. This necessitates the adoption of a highly conservative approach when constructing flexibility models for individual DERs. When aggregating these DERs, this conservativeness can lead to a significant underestimation of the aggregated flexibility region or even potentially render the aggregation process infeasible. For example, the homothetic polytope-based Minkowski sum aggregation method

This work was supported in part by Beijing Municipal Science and Technology Commission, Administrative Commission of Zhongguancun Science Park under Grant Z221100000222022; in part by the China Scholarship Council under Award 202206210220; in part by the Swiss Federal Office of Energy's "SWEET" programme and performed in the PATHFNDR consortium.

described in [8] may face infeasibility issues when the connection times of two EVs do not overlap. Fortunately, predicting the aggregated flexibility parameters of many DERs, including the uncertainty, is easier due to the complementarity among the uncertainties of DERs (Law of large numbers). Therefore, we opt to define a deterministic aggregation model first and then introduce stochasticity into this model.

The modeling of aggregated flexibility is known to be NP-hard [9]. Prior research [9]–[14] has proposed various approximated aggregation models, including outer and inner approximations, to reduce the computational complexity of the exact aggregation model. An outer approximation contains the region of the exact aggregation model, which leads to an optimistic prediction of the available aggregated flexibility. A straightforward way to construct the outer approximation is to choose a subset of the constraints in the exact model, e.g., constraints on the aggregated power and energy [9]–[11]. On the other hand, an inner approximation determines a region contained by the region of the exact aggregation model, which is thus a conservative evaluation of the aggregated flexibility. Inner approximation models are usually constructed by finding the largest inscribed polytope, with a prescribed shape, in the region of the exact aggregation model [12]–[14]. Note that the inner approximations usually lead to a conservative flexibility region, which inadvertently is robust with respect to the potential uncertainty. However, the conservativeness of this robustness is not properly quantified, so further work on uncertainty modeling based on inner approximations is still necessary.

In this paper, we choose chance-constrained programming (CCP) as our approach to model the power-energy flexibility boundaries. Many studies apply a Conditional Value-at-Risk (CVaR) approximation to generate a tractable approximation of CCPs, which has been widely used in power system applications, e.g., dispatch problems [15], [16] and optimal power flow [17], [18], due to its simplicity and convexity preservation. Theoretically, the decision made by the CVaR approximated CCP is more conservative than the result of the original CCP [19]. However, when CVaR is applied to chance constraints with double-sided inequalities, e.g., the constraints in the flexibility model of DERs, it has deficiencies because its inherent conservativeness can potentially transform an originally feasible chance constraint into an infeasible reformulation. In this paper, we proposed an uncertainty modeling method for the aggregated flexibility based on ALSO-X+ [20], which is, in theory, also a conservative approximation of CCPs but is less conservative than the decisions from CVaR-based approaches. This method is expected to solve the over-conservativeness and infeasibility problems of CVaR, thereby facilitating the employment of DERs' flexibility in power systems.

Hence, in this paper, we propose a stochastic flexibility modeling and identification method for aggregated DERs. We formulate the deterministic aggregated flexibility as a power-energy boundary model, which can be either an outer or inner approximation depending on its boundary parameters [9], [14]. Using the historical data of operational patterns of DERs to generate samples of the boundary parameters in the aggregated flexibility model, we leverage the sample-based version of ALSO-X+ approximated CCP to model the uncertainty of power-energy boundaries. The proposed aggregation model serves as an input to the decision-making at the aggregator or a higher level (e.g., the transmission level). At this level, there is always a tradeoff to be made between the computational efficiency of the decision problem and the modeling details of individual DERs. The proposed method ensures that the aggregated power profile determined by the upper layer can be disaggregated to each DER with a small error for execution without modeling the complete DER information at the aggregator level. In numerical tests, we compare the cost and risk of using ALSO-X+ and CVaR to approximate the CCP, as well as the disaggregation errors of inner and outer approximated aggregation models. The simulation results and discussions provide insights into the performance of these modeling approaches and enable DER aggregators to make informed decisions about the choice of their flexibility models.

II. Deterministic Aggregated Flexibility Model

In the proposed approach, the deterministic flexibility aggregation model serves as the basis for the uncertainty modeling. This section starts with the individual flexibility model of DER and then presents the deterministic flexibility aggregation models.

A. Flexibility Modeling of Individual DERs

Although different DERs have various operational patterns, their flexibility can be uniformly described by a power-energy boundary model [10]. We now consider the operational period to have T time slots with the length of ΔT. The flexibility of each DER can be formulated as the following constraints:

$$\underline{p}_{i,t} \leq p_{i,t} \leq \overline{p}_{i,t}, \forall t \in [T], \forall i \in \mathcal{N}, \tag{1a}$$

$$\underline{e}_{i,t} \leq \Delta T \sum\nolimits_{\tau=1}^{t} p_{i,\tau} \leq \overline{e}_{i,t}, \forall t \in [T], \forall i \in \mathcal{N}, \tag{1b}$$

where $i/\mathcal{N}$ denotes the indices/set of DERs, $|\mathcal{N}| = N$, $[T] \triangleq \{1, 2, \cdots, T\}$; $p_{i,t} \in \mathbb{R}$ denotes the power consumption variable of DER i at time t; $\underline{p}_{i,t} \in \mathbb{R}$, $\overline{p}_{i,t} \in \mathbb{R}$, $\underline{e}_{i,t} \in \mathbb{R}$, and $\overline{e}_{i,t} \in \mathbb{R}$ are the power and energy boundary parameters of DER i at time t. The power-energy boundary model (1) describes the DER's flexibility by limiting its maximal and minimal power profiles and the fastest and slowest energy consumption trajectories.

B. Outer and Inner Approximated Aggregation Models

A flexibility aggregation model refers to a feasible region that contains all possible values for the aggregated power variable $P_t \triangleq \sum_{i \in \mathcal{N}} p_{i,t}, \forall t \in [T]$. For the number of T time slots, the total number of constraints in an exact aggregation model is $2(2^T - 1)$ if we simply combine the flexibility regions (1) of all individual DERs [9]. This exponentially growing complexity with respect to the number of time steps leads to high computational costs, and it is unsuitable for a large-scale

multi-period decision problem. To reduce the computational complexity, we use the approximate power-energy boundary model to describe the aggregated flexibility of multiple DERs, as follows:

$$\underline{P}_t \le P_t \le \overline{P}_t, \quad \forall t \in [T], \tag{2a}$$

$$\underline{E}_t \le \Delta T \sum\nolimits_{\tau=1}^{t} P_\tau \le \overline{E}_t, \quad \forall t \in [T], \tag{2b}$$

where $\underline{P}_t \in \mathbb{R}$, $\overline{P}_t \in \mathbb{R}$, $\underline{E}_t \in \mathbb{R}$, and $\overline{E}_t \in \mathbb{R}$ are the power and energy boundary parameters of the aggregator at time t, calculated based on the individual boundary parameters.

The aggregator model (2) can be either an outer or inner approximation depending on its boundary parameters. As for the outer approximation, the parameters can be defined by directly summing up the individual boundary parameters as follows:
$\forall t \in [T]$:

$$\underline{P}_t^{\text{out}} \triangleq \sum\nolimits_{i\in\mathcal{N}} \underline{p}_{i,t}, \quad \overline{P}_t^{\text{out}} \triangleq \sum\nolimits_{i\in\mathcal{N}} \overline{p}_{i,t},$$

$$\underline{E}_t^{\text{out}} \triangleq \sum\nolimits_{i\in\mathcal{N}} \underline{e}_{i,t}, \quad \overline{E}_t^{\text{out}} \triangleq \sum\nolimits_{i\in\mathcal{N}} \overline{e}_{i,t}.$$

The power-energy boundary constraints in (2) specified by $(\underline{P}_t^{\text{out}}, \overline{P}_t^{\text{out}}, \underline{E}_t^{\text{out}}, \overline{E}_t^{\text{out}}), \forall t \in [T]$ are in fact a subset of the constraints in the exact aggregation model, hence, the region determined by these constraints contains the exact aggregated feasible region, resulting in an outer approximation model [9].

Boundary parameters of an inner approximation model defined by $(\underline{P}_t^{\text{in}}, \overline{P}_t^{\text{in}}, \underline{E}_t^{\text{in}}, \overline{E}_t^{\text{in}}), \forall t \in [T]$ are calculated by iteratively shrinking the boundaries of the outer approximation based on its vertices outside the exact aggregation model [14]. Generally speaking, the power and energy envelopes of the inner approximation model are narrower than those of the outer approximation model, ensuring that the feasible region defined by these ranges is inside the exact model. This fact makes the inner approximation model more conservative than the exact aggregation model, which, though not designed to handle uncertainty, can make the inner approximation robust to uncertain boundary parameters. However, this robustness to the uncertainty has not been properly justified by probability methods. Consequently, stochastic uncertainty modeling of these boundary parameters is still of interest.

Overall, the outer and inner approximated power-energy boundary models can both be used to describe the aggregated flexibility. The boundary parameters in the outer and inner approximation models are uncertain because they are calculated based on the individual parameters of DERs, which are affected by unpredictable factors, e.g., the arrival and departure time of EVs and the ambient temperature of HVACs. To address this uncertainty, we compute these boundary parameters based on historical datasets and then input the computed parameters as historical samples into the following uncertainty modeling.

III. Uncertainty Modeling via the ALSO-X+ Approximated CCP

In this section, we develop a stochastic model of aggregated flexibility by considering the power-energy boundary parameters in (2) as uncertain variables. For simplicity, we remove the superscripts "in" and "out" and rewrite the constraints (2) in a compact matrix form over the time horizon $[T]$, as follows:

$$\mathbf{AP} \le \tilde{\boldsymbol{\xi}},$$

where

$$\mathbf{A} \triangleq \left[\mathbf{I}, -\mathbf{I}, \mathbf{L}^\top, -\mathbf{L}^\top\right]^\top, \mathbf{P} \triangleq [P_1, P_2, ..., P_T]^\top,$$

$$\mathbf{I} \triangleq \begin{bmatrix} 1 & & & \\ & 1 & & \\ & & \ddots & \\ & & & 1 \end{bmatrix}, \ \mathbf{L} \triangleq \begin{bmatrix} 1 & & & \\ 1 & 1 & & \\ \vdots & \vdots & \ddots & \\ 1 & 1 & \cdots & 1 \end{bmatrix},$$

$$\tilde{\boldsymbol{\xi}} \triangleq \left[\overline{\mathbf{P}}^\top, -\underline{\mathbf{P}}^\top, \frac{\overline{\mathbf{E}}^\top}{\Delta T}, -\frac{\underline{\mathbf{E}}^\top}{\Delta T}\right]^\top,$$

$$\overline{\mathbf{P}} \triangleq \left[\overline{P}_1, \overline{P}_2, ..., \overline{P}_T\right]^\top, \ \underline{\mathbf{P}} \triangleq [\underline{P}_1, \underline{P}_2, ..., \underline{P}_T]^\top,$$

$$\overline{\mathbf{E}} \triangleq \left[\overline{E}_1, \overline{E}_2, ..., \overline{E}_T\right]^\top, \ \underline{\mathbf{E}} \triangleq [\underline{E}_1, \underline{E}_2, ..., \underline{E}_T]^\top.$$

The operator $(\cdot)^\top$ calculates the vector/matrix transposition. The constant coefficient matrix $\mathbf{A} \in \mathbb{R}^{4T\times T}$ and the sub-matrices $\mathbf{I} \in \mathbb{R}^{T\times T}$ and $\mathbf{L} \in \mathbb{R}^{T\times T}$ reformulate the power and energy constraints in a matrix form. The random vector $\tilde{\boldsymbol{\xi}}$ collects the uncertain power and energy boundaries with the support set $\Xi \subseteq \mathbb{R}^{4T}$.

Since this paper focuses on uncertainty modeling of power-energy boundaries, we consider the decision-making scenario of the DER aggregator: optimizing the aggregator's power profile to minimize the total electricity cost, given as follows:

$$v^* = \min_{\mathbf{P}\in\mathbb{R}^T} \mathbf{c}^\top \mathbf{P}, \tag{5a}$$

$$\text{s.t. } \mathbb{P}\left(\mathbf{AP} \le \tilde{\boldsymbol{\xi}}\right) \ge 1-\epsilon, \tag{5b}$$

where $\mathbf{c} \in \mathbb{R}^T$ denotes the time-of-use electricity prices over time period T, $\epsilon \ge 0$ is a prescribed risk level. Problem (5) is a CCP that optimizes the aggregator's total electricity cost while ensuring that all constraints in the aggregated flexibility model are simultaneously satisfied with a probability no less than $1-\epsilon$. Constraint (5b) is a joint chance constraint including $4T$ inequalities.

Note that the above CCP (5) cannot be solved directly as the distribution information $\mathbb{P}$ is unknown. As discussed in Section II, we use historical data of individual DERs' operational patterns to sample the uncertain variable $\tilde{\boldsymbol{\xi}}$. We assume that the support set Ξ is a finite set composed of a limited number of samples, i.e., $\Xi = \{\boldsymbol{\xi}_1, \boldsymbol{\xi}_2, \cdots, \boldsymbol{\xi}_n\}$ where n denotes the number of samples. Then CCP (5) can be reformulated as a tractable form via various approximation methods, for instance, the CVaR approximation, which has been widely used in the literature. However, the CVaR approximation is often over-conservative. This conservativeness has the potential of turning an originally feasible chance constraint into an infeasible reformulation, especially in the case of the uncertainty modeling of flexibility, where both the upper and lower boundaries are uncertain variables. If the approximated

chance constraint is infeasible, the aggregated power-energy envelopes will be meaningless for further decision-making.

In this paper, we adopt a recently developed stochastic optimization technique, i.e., the ALSO-X+ approximation method [20], which is less conservative than CVaR. In the ALSO-X+ method, CCP (5) is first reformulated as the following sample-based equivalent form:

$$v^* = \min v, \tag{6a}$$

$$\text{s.t. } (\mathbf{P}^*, \mathbf{s}^*, \mathbf{z}^*) = \arg\min \left\{ \begin{array}{l} \sum_{i=1}^n z_i s_i : \\ \mathbf{P} \in \mathbb{R}^T, \mathbf{s} \in \mathbb{R}^n, \mathbf{z} \in \mathbb{R}^n, \\ \mathbf{c}^\top \mathbf{P} \le v, \mathbf{0} \le \mathbf{z} \le \mathbf{1}, \mathbf{s} \ge \mathbf{0}, \\ \frac{1}{n}\sum_{i=1}^n z_i \ge 1-\epsilon, \\ \mathbf{A}\mathbf{P} - \boldsymbol{\xi}_i \le s_i, \forall 1 \le i \le n \end{array} \right\}, \tag{6b}$$

$$\sum_{i=1}^n z_i^* s_i^* = 0, \tag{6c}$$

where $\mathbf{s} \triangleq [s_1, \ldots, s_n]^\top \in \mathbb{R}^n$ is an auxiliary vector representing the relaxation on the joint chance constraint for each uncertain sample $\boldsymbol{\xi}_i$, $\mathbf{z} \triangleq [z_1, \ldots, z_n]^\top \in \mathbb{R}^n$ is also an auxiliary vector representing the activation level of the relaxation $\mathbf{s}$. We use this bi-level optimization problem (6) to equivalently (in the sense of a finite support set Ξ) represent CCP (5). The upper-level problem determines the objective value v. The lower-level problem (6b) minimizes the total activated relaxation on the joint chance constraint under a given v. Constraint (6c) ensures that the original joint chance constraint (5b) is satisfied. This reformulation based on the ALSO-X+ model controls the confidence level of the CCP by constraining the total activation rate $\frac{1}{n}\sum_{i=1}^n z_i$ to no less than $1-\epsilon$ in the lower-level optimization (6b) and checking whether the total relaxation of all activated constraints equals to zero via constraint (6c).

There are two challenges in solving problem (6): one is how to calculate the bi-level optimization, and the other is how to solve the lower-level problem (6b) including the bilinear term $z_i s_i$ in the objective. For the first challenge, since v is the only variable in the upper-level problem, a bisection can be used to find v^*. For the second, the lower-level problem is solved by an alternating optimization process, that is, to iteratively fix either $\mathbf{z}$ or $\mathbf{s}$ to solve the other. The proposed optimal dispatch decision searching algorithm based on ALSO-X+ with uncertain flexibility modeling of DERs is summarized in Algorithm 1.

The outer loop of Algorithm 1 is a bisection on objective v, with the stopping criterion of a small enough gap between the upper and lower boundaries v^{U} and v^{L}. When the ALSO-X+ approximated CCP is infeasible, the objective v will converge to the upper bound v^{U}. The number of iterations required for the outer loop is proportional to $\log(v^{\mathrm{U}} - v^{\mathrm{L}})$. The inner loop solves problem (6b) by an alternating optimization with two stopping criteria, $\Gamma^k = 0$ and $\Delta < \delta_2$. The first criterion, $\Gamma^k = 0$, means that the lower-level problem (6b) has already reached the optimum under the current objective function value v and the solution $\mathbf{P}^k$, because the lower bound of its objective is 0. The second criterion, $\Delta < \delta_2$, means that the reduction of the lower objective is less than δ_2. The inner loop has a convergence guarantee because its objective is monotonically non-increasing and has a lower bound of 0. In the end, the output optimizer $\mathbf{P}^k$ of Algorithm 1 is a conservatively approximated solution of the original CCP, but less conservative than the solution calculated by CVaR.

Algorithm 1 The ALSO-X+ algorithm for approximately solving CCP (5)

Input: Tolerence level δ_1, δ_2, upper and lower boundaries of the objective value v^{U} and v^{L}

while $v^{\mathrm{U}} - v^{\mathrm{L}} > \delta_1$ **do**
  Let $v = \frac{(v^{\mathrm{U}} + v^{\mathrm{L}})}{2}$, $\mathbf{s}^0 = \boldsymbol{\infty}$, $\mathbf{z}^0 = \mathbf{1}$, $\Gamma^0 = \infty$, $k = 0$
  repeat
    Solve

$$\left(\mathbf{P}^{k+1}, \mathbf{s}^{k+1}\right) = \arg\min \left\{ \begin{array}{l} \sum_{i=1}^n z_i^k s_i : \\ \mathbf{c}^\top \mathbf{P} \le v, \mathbf{s} \ge \mathbf{0}, \\ \forall i \in \{1, 2, ..., n\} : \\ \mathbf{A}\mathbf{P} - \boldsymbol{\xi}_i \le s_i \end{array} \right\}$$

    Solve

$$\mathbf{z}^{k+1} = \arg\min \left\{ \begin{array}{l} \sum_{i=1}^n z_i s_i^{k+1} : \\ \mathbf{0} \le \mathbf{z} \le \mathbf{1}, \\ \frac{1}{n}\sum_{i=1}^n z_i \ge 1-\epsilon \end{array} \right\}$$

    Let $k = k+1$, $\Gamma^k = \sum_{i=1}^n z_i^k s_i^k$, $\Delta = \left|\Gamma^k - \Gamma^{k-1}\right|$
  until $\Gamma^k = 0$ or $\Delta < \delta_2$
  Let $v^{\mathrm{U}} = v$ if $\Gamma = 0$; otherwise, let $v^{\mathrm{L}} = v$
end while

Output: An optimizer $\mathbf{P}^k$ and its objective v^*

IV. Numerical Studies

In this section, we conduct numerical studies to compare the proposed method and the CVaR-based approach[1], with respect to the cost efficiency, the conservativeness of decisions, and the feasibility. Moreover, as an alternative basis for uncertainty modeling, the outer and inner approximated flexibility aggregation models are also compared in terms of costs and disaggregation errors.

A. System Settings

We consider an aggregator with two types of DERs: EVs and HVACs. Different cases are generated by adjusting the numbers of EVs and HVACs in the aggregator. The arrival and departure time and initial and expected states-of-charge of EVs and thermal resistance and capacity of HVACs are generated by random sampling, with the detailed parameters being the same as in [9]. We consider the day-ahead optimization of the aggregator with a time horizon of 24 hours and an interval of $\Delta T = 1$ hour. The electricity price profile $\mathbf{c}$ is taken from the NordPool day-ahead market price in France on August 11th,

[1]The detailed formulation of the CVaR approximated CCP in this case study can be found in [19].

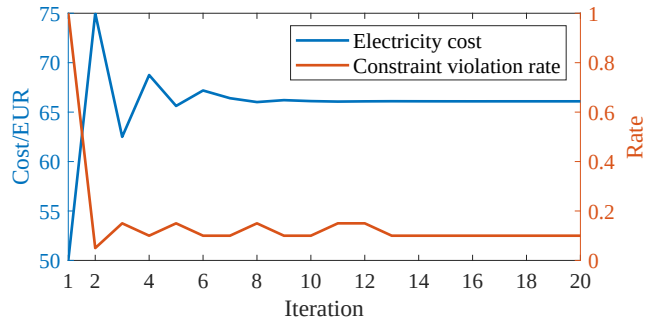

Fig. 1. Changes in electricity cost and constraint violation rate during the outer-loop iteration.

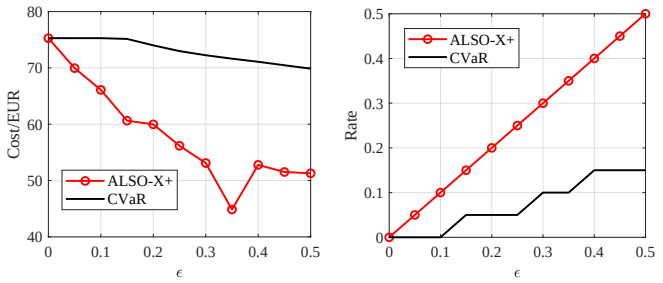

(a) Electricity cost. (b) Constraint violation rate.

Fig. 2. Results of ALSO-X+ and CVaR under different ϵ when the aggregator has 20 EVs and 20 HVACs.

2023 [21]. The number of uncertain samples in the support set is $n = 20$, and the convergence tolerances are set to $\delta_1 = \delta_2 = 10^{-4}$.

All simulations are performed on a laptop with an 8-core Intel i7-1165G7 CPU and 32-GB RAM, programmed by `MATLAB` [22], and solved by `Cplex` [23].

B. Convergence of the ALSO-X+ Algorithm

In the first case study, we consider an aggregator having 20 EVs and 20 HVACs and set the risk level $\epsilon = 0.1$. The initial upper and lower boundaries of the objective are $v^{\mathrm{U}} = 100$ EUR, and $v^{\mathrm{L}} = 0$. Based on the outer approximated power-energy boundary model that is defined by $(\underline{P}_t^{\text{out}}, \overline{P}_t^{\text{out}}, \underline{E}_t^{\text{out}}, \overline{E}_t^{\text{out}}), \forall t \in [T]$, we implement the ALSO-X+ algorithm to solve CCP (5).

Fig. 1 shows the changes in the electricity cost and the *constraint violation rate*[2] at each outer-loop iteration. It can be seen that the changes in the electricity cost and the constraint violation rate gradually decrease as the iteration continues. Convergence is achieved after 20 iterations, taking 1.4410 seconds, which meets the requirements for day-ahead decision-making problems. In intraday decision-making, the number of time slots considered is fewer than in day-ahead decision-making (e.g., the North China Power Grid looks forward 1 hour with a 15-minute interval in intraday dispatch, so aggregators there consider four slots in their intraday decision-making process), resulting in fewer constraints in the flexibility model and less computation time. Moreover, the time required for this iterative computation process does not increase with the number of DERs since the uncertainty modeling is based on the aggregated flexibility model of DERs, which enables the high scalability of the proposed method. In the final solution, the aggregator's electricity cost is 66.09 EUR, and the constraint violation rate reaches the pre-set risk level of 0.1. These results show that the ALSO-X+ algorithm can converge quickly and is able to control the risk level precisely.

C. Comparison between ALSO-X+ and CVaR

Following the configuration of the aggregator and the outer approximated flexibility aggregation model as in the previous subsection, we use both ALSO-X+ and CVaR to approximately solve CCP (5) under different risk levels ϵ.

Fig. 2 shows the electricity cost and the constraint violation rate calculated by the two methods. In general, cost decreases with the increase of the risk level ϵ. An exception occurs when the risk level $\epsilon = 0.35$, where ALSO-X+ identifies a solution with a lower cost than for $\epsilon = 0.4$. This variability in results is due to the ALSO-X+ algorithm's design to compute approximate solutions for CCPs, and a better approximation is found in the case of $\epsilon = 0.35$. Nonetheless, we emphasize that, with a theoretical guarantee [20], the solution obtained by ALSO-X+ will never be more conservative than that calculated by CVaR at the same risk level ϵ. Empirical evidence in Fig. 2(b) shows that the constraint violation rate of ALSO-X+ is precisely controlled at the predetermined risk level ϵ, whereas the violation rate for CVaR is significantly lower than the pre-set value. This phenomenon demonstrates the inherent conservativeness of CVaR, which directly leads to higher costs calculated by CVaR compared to ALSO-X+ for an identical risk level ϵ, shown in Fig. 2(a). These results verify the advantages of the ALSO-X+ algorithm.

Now, we change the number of DERs in the aggregator to 10 EVs and 30 HVACs. In this case, several upper energy boundary samples are lower than the highest lower boundary, as shown in Fig. 3, which can lead to potential infeasibility of the optimization problem. Samples of the power boundaries are not shown here since energy boundary samples are enough to explain the crossover of the upper and lower boundaries.

Again, we use the ALSO-X+ and CVaR approximations to solve CCP (5). The obtained costs and constraint violation rates under different risk levels ϵ are shown in Fig. 4. It is observed that the ALSO-X+ approximated CCP is feasible when $\epsilon \geq 0.05$, while the CVaR approximated CCP stays infeasible until $\epsilon \geq 0.25$. Hence, the ALSO-X+ approximation enables a wider adjustment range for the aggregator's cost and constraint violation rates compared to the CVaR approximation. Again, as pointed out in the first case, even when the constraint violation rate is the same, for example, $\epsilon = 0.05$, the cost calculated by the ALSO-X+ approximation is still lower than the costs calculated by the CVaR approximation.

Finally, we test a case of 30 EVs and 10 HVACs, where there are more crossovers between the samples of the upper

[2]The constraint violation rate is measured by counting that for how many i-s in $\{1, 2, ..., n\}$, any line in constraint $\mathbf{AP} - \boldsymbol{\xi}_i \leq 0$ is violated.

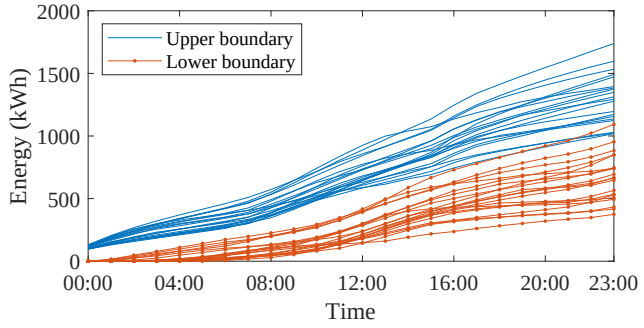

Fig. 3. Samples of the aggregated upper and lower energy boundaries. After 21:30, three sample trajectories of the upper energy boundary are lower than the highest sample trajectory of the lower energy boundary.

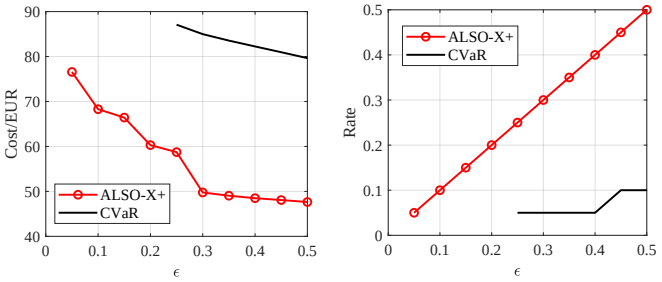

(a) Electricity cost. (b) Constraint violation rate.

Fig. 4. Results of ALSO-X+ and CVaR under different ϵ when the aggregator has 10 EVs and 30 HVACs. The missed parts of the lines are due to the infeasibility of the CCP: the ALSO-X+ approximated CCP is feasible when $\epsilon \geq 0.05$, and the CVaR approximated CCP is feasible when $\epsilon \geq 0.25$.

and lower boundaries. In this case, the CVaR approximation is infeasible independent of the value for $\epsilon \in [0, 1)$, while the ALSO-X+ approximation is feasible for $\epsilon \geq 0.3$. This result is also caused by the conservativeness of the CVaR approximation, further indicating the benefits of using the ALSO-X+ approximation rather than CVaR.

D. Comparison between the Outer and Inner Approximated Flexibility Aggregation Models

This subsection aims to compare the impact of outer and inner approximated flexibility aggregation models on the optimization results. As the superior performance of the ALSO-X+ approximation over CVaR in the term of conservativeness is already demonstrated in the previous subsection, we only use the ALSO-X+ approximation to solve CCP (5) in this subsection.

The difference between inner and outer approximated aggregation models is mainly reflected when disaggregating the total power of the aggregator into operational regions of individual DERs. Specifically, after we solve CCP (5), the obtained optimal dispatch decision $P_t^*, \forall t \in [T]$ of the aggregator should be disaggregated to each DER for execution according to their individual operational regions, which can be done by solving the below optimization problem:

$$err = \min \sum_{t=1}^{T} (P_t - P_t^*)^2, \tag{7a}$$

$$\text{s.t. } P_t = \sum_{i \in N} p_{i,t}, \forall t \in [T], \tag{7b}$$

$$\underline{p}_{i,t} \leq p_{i,t} \leq \overline{p}_{i,t}, \forall t \in [T], \forall i \in \mathcal{N}, \tag{7c}$$

$$\underline{e}_{i,t} \leq \Delta T \sum\nolimits_{\tau=1}^{t} p_{i,\tau} \leq \overline{e}_{i,t}, \forall t \in [T], \forall i \in \mathcal{N}, \tag{7d}$$

where $P_t, \forall t \in [T]$ denotes optimal aggregated dispatch power that can be disaggregated and assigned to individual DERs, and the boundary parameters $(\underline{p}_{i,t}, \overline{p}_{i,t}, \underline{e}_{i,t}, \overline{e}_{i,t})$ are specified based on the actual data of individual DERs. The objective err, called *disaggregation error*, is the squared error between the power profile $P_t, \forall t \in [T]$ that can be actually disaggregated and the optimal aggregated dispatch decision $P_t^*, \forall t \in [T]$ from Algorithm 1.

Again, we use the previous case of an aggregator with 20 EVs and 20 HVACs. The disaggregation error is quantified on a total of 50 test scenarios of individual DER information that are randomly sampled using the same parameters from which the previous sample set Ξ is generated. The disaggregation error err is normalized by

$$err_{\text{norm}} = \frac{\sqrt{err}}{\sum_{t=1}^{T} |P_t^*|}$$

to eliminate the influence of the absolute power value.

Fig. 5 shows the tradeoff between the cost and disaggregation error using both the outer and inner approximated flexibility aggregation models for uncertainty modeling. Results of different costs and disaggregation errors are obtained by adjusting the risk parameter ϵ in the optimization problem. In general, the decrease in error is accompanied by an increase in cost. Within the cost range of the inner approximation, roughly between 43 EUR and 70 EUR, the disaggregation error of the outer approximation is similar to that of the inner approximation. However, the outer approximation has a wider range of costs and disaggregation errors than the inner approximation. From the perspective of being able to choose a tradeoff between error and cost efficiency, the outer approximated flexibility aggregation model is more advantageous as a choice of uncertainty modeling in this case.

When adding additionally a 25 kW/100 kWh battery and a 30 kW PV to the 20 EVs and 20 HVACs, we observe different results. Following the above simulation steps, we also calculate the relationship between the cost and disaggregation error, as shown in Fig. 6. Although the range of the cost and error of the outer approximation is still wider than that of the inner approximation, the inner approximation has a lower disaggregation error than the outer approximation at the same cost. Hence, in this test case, the inner approximation is more advantageous as an alternative to modeling the uncertainty of power-energy boundaries.

In addition to these two cases, we have also tested other combinations of DERs, arriving at conclusions similar to

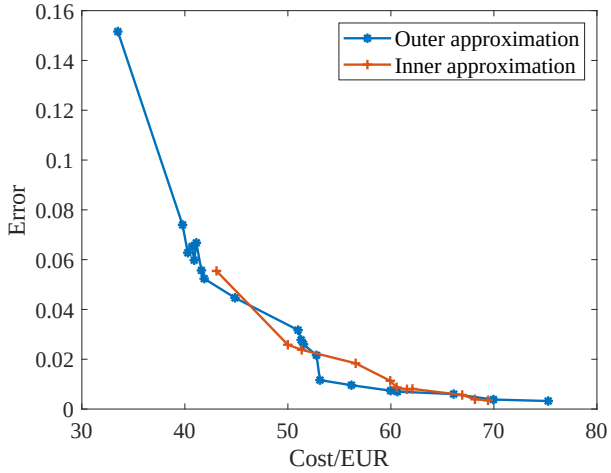

Fig. 5. Relationship between cost and disaggregation error using the outer and inner approximated power-energy boundary model as the basis of uncertainty modeling when the aggregator has 20 EVs and 20 HVACs.

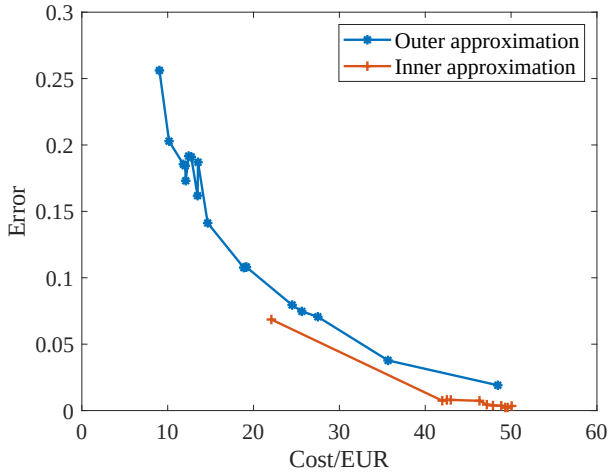

Fig. 6. Relationship between cost and disaggregation error using the outer and inner approximated power-energy boundary model as the basis of uncertainty modeling when the aggregator has 20 EVs, 20 HVACs, a 25kW/100kWh DESS, and 30 kW installed PV.

one of the two aforementioned results. In summary, there is no definitive conclusion on whether the inner or outer approximation model is superior for modeling uncertainty under different compositions of aggregators. Therefore, we recommend that the aggregator tests both the inner and outer approximations to model the aggregated flexibility envelops and evaluates their performance with respect to cost efficiency and disaggregation error.

V. Conclusions

This paper proposes an uncertainty modeling method for the aggregated flexibility of DERs. We use the power-energy boundary model with both inner and outer approximated parameters to describe the aggregated flexibility of multiple DERs. These boundary parameters are uncertain variables because they are affected by all DERs in the aggregator. Modeling the aggregator's optimization with uncertainty as a CCP, the ALSO-X+ algorithm is used to solve it approximately to get the reference load profile of the aggregator. The ALSO-X+ approximation is less conservative than the conventional CVaR approximation, enabling a wider range for cost and risk (i.e., the rate of constraint violation) and solving the infeasibility problem of CVaR.

A potential limitation in the simulations is that we used electricity price data and DER parameters from different sources. However, consistent data was not available at this stage of the work. Nevertheless, the presented simulations can still be used to verify the advantages of the proposed method over CVaR.

The proposed uncertainty modeling approach has a broad application to different power system operation problems, such as the aggregator's bidding strategy in power markets, the ancillary provision with multiple DER aggregators, and others. Future work will focus on developing the proposed flexibility modeling for the different application scenarios according to their distinct attributes and requirements.

References

[1] A. Cherp, V. Vinichenko, J. Tosun, J. A. Gordon, and J. Jewell, "National growth dynamics of wind and solar power compared to the growth required for global climate targets," *Nature Energy*, vol. 6, no. 7, pp. 742–754, 2021.

[2] F. Plaum, R. Ahmadiahangar, A. Rosin, and J. Kilter, "Aggregated demand-side energy flexibility: A comprehensive review on characterization, forecasting and market prospects," *Energy Reports*, vol. 8, pp. 9344–9362, 2022.

[3] W. Sun, F. Neumann, and G. P. Harrison, "Robust scheduling of electric vehicle charging in LV distribution networks under uncertainty," *IEEE Transactions on Industry Applications*, vol. 56, no. 5, pp. 5785–5795, 2020.

[4] Y. Wang, Q. Zeng, Z. Tian, Y. Du, P. Zeng, and L. Jiang, "Distributionally robust energy consumption scheduling of HVAC considering the uncertainty of outdoor temperature and human activities," *CSEE Journal of Power and Energy Systems*, 2022.

[5] PJM Manual 11: Energy and Ancillary Services Market Operations. [Online]. Available: https://www.pjm.com/-/media/documents/manuals/m11.ashx

[6] National Energy Administration North China Regulatory Bureau. (2020, Dec) Third-party independent entities participate in North China Electric Power Balancing Ancillary Service Market Rules (Trial, 2020 Edition). [Online]. Available: https://shupeidian.bjx.com.cn/html/20201211/1121676.shtml

[7] S. Wang and W. Wu, "Aggregate flexibility of virtual power plants with temporal coupling constraints," *IEEE Transactions on Smart Grid*, vol. 12, no. 6, pp. 5043–5051, 2021.

[8] Z. Yi, Y. Xu, W. Gu, L. Yang, and H. Sun, "Aggregate operation model for numerous small-capacity distributed energy resources considering uncertainty," *IEEE Transactions on Smart Grid*, vol. 12, no. 5, pp. 4208–4224, 2021.

[9] Y. Wen, Z. Hu, S. You, and X. Duan, "Aggregate feasible region of DERs: Exact formulation and approximate models," *IEEE Trans. Smart Grid*, vol. 13, no. 6, pp. 4405–4423, 2022.

[10] Z. Xu, D. S. Callaway, Z. Hu, and Y. Song, "Hierarchical coordination of heterogeneous flexible loads," *IEEE Transactions on Power Systems*, vol. 31, no. 6, pp. 4206–4216, 2016.

[11] L. Wang, J. Kwon, N. Schulz, and Z. Zhou, "Evaluation of aggregated ev flexibility with tso-dso coordination," *IEEE Transactions on Sustainable Energy*, vol. 13, no. 4, pp. 2304–2315, 2022.

[12] X. Chen, E. Dall'Anese, C. Zhao, and N. Li, "Aggregate power flexibility in unbalanced distribution systems," *IEEE Transactions on Smart Grid*, vol. 11, no. 1, pp. 258–269, 2019.

[13] D. Yan, C. Ma, and Y. Chen, "Distributed coordination of charging stations considering aggregate ev power flexibility," *IEEE Transactions on Sustainable Energy*, vol. 14, no. 1, pp. 356–370, 2022.
[14] Y. Wen, Z. Hu, J. He, and Y. Guo, "Improved inner approximation for aggregating power flexibility in active distribution networks and its applications," *arXiv preprint arXiv:2303.01691*, 2023.
[15] J. Zhai, Y. Jiang, Y. Shi, C. N. Jones, and X.-P. Zhang, "Distributionally robust joint chance-constrained dispatch for integrated transmission-distribution systems via distributed optimization," *IEEE Transactions on Smart Grid*, vol. 13, no. 3, pp. 2132–2147, May 2022.
[16] C. Ordoudis, V. A. Nguyen, D. Kuhn, and P. Pinson, "Energy and reserve dispatch with distributionally robust joint chance constraints," *Operations Research Letters*, vol. 49, no. 3, pp. 291–299, May 2021.
[17] Y. Guo, K. Baker, E. Dall'Anese, Z. Hu, and T. H. Summers, "Data-based distributionally robust stochastic optimal power flow—Part I: methodologies," *IEEE Transactions on Power Systems*, vol. 34, no. 2, pp. 1483–1492, 2018.
[18] R. A. Jabr, "Distributionally robust CVaR constraints for power flow optimization," *IEEE Transactions on Power Systems*, vol. 35, no. 5, pp. 3764–3773, 2020.
[19] W. Xie, "On Distributionally Robust Chance Constrained Programs with Wasserstein Distance," *Mathematical Programming*, vol. 186, no. 1, pp. 115–155, Mar. 2021.
[20] N. Jiang and W. Xie, "ALSO-X and ALSO-X+: Better convex approximations for chance constrained programs," *Operations Research*, vol. 70, no. 6, pp. 3581–3600, Nov. 2022.
[21] Nord Pool. Day-ahead prices: FR - France. [Online]. Available: https://www.nordpoolgroup.com/en/Market-data1/Dayahead/Area-Prices/fr/hourly
[22] The MathWorks Inc., "MATLAB version: 9.13.0 (R2022b)," Natick, Massachusetts, United States, 2022. [Online]. Available: https://www.mathworks.com
[23] IBM, "IBM ILOG CPLEX Optimizer," Armonk, New York, United States, 2022. [Online]. Available: https://www.ibm.com/analytics/cplex-optimizer